Medical Physics
The International Journal of Medical Physics Research and Practice

Toward a clinical application of ex situ boron neutron capture therapy for lung tumors at the RA-3 reactor in Argentina

R. O. Farías, M. A. Garabalino, S. Ferraris, J. Santa María, O. Rovati, F. Lange, V. A. Trivillin, A. Monti Hughes, E. C. C. Pozzi, S. I. Thorp, P. Curotto, M. E. Miller, G. A. Santa Cruz, S. Bortolussi, S. Altieri, A. M. Portu, G. Saint Martin, A. E. Schwint, and S. J. González

Citation: Medical Physics **42**, 4161 (2015); doi: 10.1118/1.4922158
View online: http://dx.doi.org/10.1118/1.4922158
View Table of Contents: http://scitation.aip.org/content/aapm/journal/medphys/42/7?ver=pdfcov
Published by the American Association of Physicists in Medicine

Toward a clinical application of *ex situ* boron neutron capture therapy for lung tumors at the RA-3 reactor in Argentina

R. O. Farías[a)]
Comisión Nacional de Energía Atómica (CNEA), San Martín 1650, Argentina and Consejo Nacional de Investigaciones Científicas y Técnicas (CONICET), Buenos Aires 1033, Argentina

M. A. Garabalino[a)]
Comisión Nacional de Energía Atómica (CNEA), San Martín 1650, Argentina

S. Ferraris, J. Santa María, O. Rovati, and F. Lange
CIDME, Universidad Maimónides, Buenos Aires 1405, Argentina

V. A. Trivillin
Comisión Nacional de Energía Atómica (CNEA), San Martín 1650, Argentina and Consejo Nacional de Investigaciones Científicas y Técnicas (CONICET), Buenos Aires 1033, Argentina

A. Monti Hughes, E. C. C. Pozzi, S. I. Thorp, P. Curotto, M. E. Miller, and G. A. Santa Cruz
Comisión Nacional de Energía Atómica (CNEA), San Martín 1650, Argentina

S. Bortolussi
Istituto Nazionale di Fisica Nucleare, Sezione di Pavia 27100, Italy

S. Altieri
Istituto Nazionale di Fisica Nucleare, Sezione di Pavia 27100, Italy and Dipartimento di Fisica, Università di Pavia, Pavia 27100, Italy

A. M. Portu
Comisión Nacional de Energía Atómica (CNEA), San Martín 1650, Argentina and Consejo Nacional de Investigaciones Científicas y Técnicas (CONICET), Buenos Aires 1033, Argentina

G. Saint Martin
Comisión Nacional de Energía Atómica (CNEA), San Martín 1650, Argentina

A. E. Schwint and S. J. González[b)]
Comisión Nacional de Energía Atómica (CNEA), San Martín 1650, Argentina and Consejo Nacional de Investigaciones Científicas y Técnicas (CONICET), Buenos Aires 1033, Argentina

(Received 31 October 2014; revised 21 May 2015; accepted for publication 25 May 2015; published 16 June 2015)

Purpose: Many types of lung tumors have a very poor prognosis due to their spread in the whole organ volume. The fact that boron neutron capture therapy (BNCT) would allow for selective targeting of all the nodules regardless of their position, prompted a preclinical feasibility study of *ex situ* BNCT at the thermal neutron facility of RA-3 reactor in the province of Buenos Aires, Argentina. (L)-4p-dihydroxy-borylphenylalanine fructose complex (BPA-F) biodistribution studies in an adult sheep model and computational dosimetry for a human explanted lung were performed to evaluate the feasibility and the therapeutic potential of *ex situ* BNCT.

Methods: Two kinds of boron biodistribution studies were carried out in the healthy sheep: a set of pharmacokinetic studies without lung excision, and a set that consisted of evaluation of boron concentration in the explanted and perfused lung. In order to assess the feasibility of the clinical application of *ex situ* BNCT at RA-3, a case of multiple lung metastases was analyzed. A detailed computational representation of the geometry of the lung was built based on a real collapsed human lung. Dosimetric calculations and dose limiting considerations were based on the experimental results from the adult sheep, and on the most suitable information published in the literature. In addition, a workable treatment plan was considered to assess the clinical application in a realistic scenario.

Results: Concentration-time profiles for the normal sheep showed that the boron kinetics in blood, lung, and skin would adequately represent the boron behavior and absolute uptake expected in human tissues. Results strongly suggest that the distribution of the boron compound is spatially homogeneous in the lung. A constant lung-to-blood ratio of 1.3 ± 0.1 was observed from 80 min after the end of BPA-F infusion. The fact that this ratio remains constant during time would allow the blood boron concentration to be used as a surrogate and indirect quantification of the estimated value in the explanted healthy lung. The proposed preclinical animal model allowed for the study of the explanted lung. As expected, the boron concentration values fell as a result of the application of the preservation protocol required to preserve the lung function. The distribution of the boron concentration retention

factor was obtained for healthy lung, with a mean value of 0.46 ± 0.14 consistent with that reported for metastatic colon carcinoma model in rat perfused lung. Considering the human lung model and suitable tumor control probability for lung cancer, a promising average fraction of controlled lesions higher than 85% was obtained even for a low tumor-to-normal boron concentration ratio of 2.
Conclusions: This work reports for the first time data supporting the validity of the ovine model as an adequate human surrogate in terms of boron kinetics and uptake in clinically relevant tissues. Collectively, the results and analysis presented would strongly suggest that *ex situ* whole lung BNCT irradiation is a feasible and highly promising technique that could greatly contribute to the treatment of metastatic lung disease in those patients without extrapulmonary spread, increasing not only the expected overall survival but also the resulting quality of life. [http://dx.doi.org/10.1118/1.4922158]

Key words: BNCT, *ex situ* irradiation, lung tumors, BPA-F, pharmacokinetics

1. INTRODUCTION

Boron neutron capture therapy (BNCT) is a binary treatment modality that combines irradiation with a thermal or epithermal neutron beam following the administration of tumor-seeking, boron-containing drugs to produce selective irradiation of tumor tissue. The high-linear energy transfer (LET) α particles and ^{7}Li nuclei emitted during the capture of a thermal neutron by a ^{10}B nucleus have a range of approximately 5–9 μm in tissue and are known to have a high relative biological effectiveness (RBE). In this way, BNCT would potentially target neoplastic tissue selectively, mostly sparing normal tissue.[1] Clinical studies of BNCT for glioblastoma multiforme and/or melanoma and, more recently, head and neck tumors and liver metastases have been performed or are underway in the US, Japan, Italy, Finland, Sweden, The Netherlands, Argentina, Czech Republic, and Taiwan.[2–4] Some of the more recent work has also focused on novel tumor targets.[2] In the last few years, the feasibility of BNCT has been assessed in patients with treatment-resistant head and neck tumors[5,6] and malignant mesothelioma.[7,8] Based on a novel *ex situ* protocol, consisting in the irradiation of an explanted organ followed by surgical reimplant in the patient, BNCT has been applied also to treat nonresectable multifocal bilobular metastases in liver.[3,9]

On the basis of this clinical experience, a multi-institutional research project, integrated by the National Atomic Energy Commission (CNEA), Maimónides University (UM) and with the collaboration of national medical institutions, is being carried out with the main purpose of assessing the feasibility of BNCT for the treatment of disseminated lung tumors using the *ex situ* technique.

The lung is the main and sometimes the only metastatic site for many tumors.[10] In advanced disease stage, metastases can be multiple, and in these cases, the standard treatment is mainly palliative (based on chemotherapy), resulting in less than 10% survival rate at 5 yr.[11] Several metastatic diseases are confined to lung volume, without extrapulmonary invasion (i.e., oligometastatic disease, Wilm's sarcoma lung metastases, and Ewing's sarcoma lung metastasis). In these scenarios, a BNCT lung *ex situ* protocol would be potentially therapeutic, enabling the delivery of a therapeutic dose to the tumor while preserving healthy lung functionality.[12,13]

The proposed *ex situ* lung protocol is based on the one applied in Italy for the treatment of liver metastases.[3,9] The boron compound is administered to the patient; the lung is then removed, perfused, and kept in a preservation solution (PS) to guarantee its functionality. Subsequently, the isolated lung is irradiated while the patient is kept stable in the operating room. After irradiation, the treated organ is finally reimplanted. This procedure presents several aspects of interest. Given that BNCT is based on biochemical targeting combined with high LET radiation, the *ex situ* technique enables irradiation of the whole volume, maximizing the dose delivered to the nodules regardless of their position and/or shape. Moreover, a whole lung irradiation (WLI) increases the probability of successfully treating the microscopic disease. The rest of the body, including the very radiosensitive organs present in the thorax, is spared from the irradiation effects. Furthermore, the autotransplant technique avoids the issue of organ rejection related to the allotransplantation procedures.

In order to apply *ex situ* BNCT for the treatment of lung tumors in patients, several procedures have to be optimized and to date nonexistent information collected. Thus, the research project has been divided into two stages. Stage I is a preclinical phase employing a large animal model (i.e., adult sheep) to set up the surgical procedure, to study the boron compound biodistribution in lung and other tissues of interest, and to determine the healthy lung toxicity caused by WLI in a mixed neutron-photon field. Stage II has the clinical application as the final goal, and focuses on the dosimetric assessment in the human explanted lung, taking into account the boron concentrations and the dose constraints determined in the first stage.

These two stages are meant to prove the feasibility of the therapeutic strategy and to assess all the necessary conditions to irradiate an explanted human lung with nonoperable metastases. The irradiation of the human lung is planned at the RA-3 reactor in Ezeiza (Province of Buenos Aires), which has a suitable thermal neutron facility.[14]

As the results of Stage I are functional and necessary for the development of Stage II, the paper reports materials, methods, and results for the two stages sequentially. In particular, this work presents the boron concentration-time profiles using the (L)-4p-dihydroxy-borylphenylalanine fructose complex (BPA-F) in the normal adult sheep lung, in addition to the

BPA-F retention studies after organ explantation and perfusion with preservation solution. Based on available dose constraints and findings of Stage I, the computational dosimetry was analyzed and clinical treatment assessment in humans was performed. Specifically, the spatial dosimetry and the tumor control probability (TCP) associated to the *ex situ* irradiation in human lung at the RA-3 thermal column central facility (TCCF) are reported and discussed.

2. STAGE I: PRECLINICAL STUDIES BASED ON THE NORMAL LUNG SHEEP MODEL

2.A. Materials and methods

2.A.1. General procedure for ex situ BNCT

The *ex situ* protocol implies a number of steps that must be synchronously performed to reach an optimal outcome. The procedure starts in the operating room, where the animal is prepared for a transplant surgery. The infusion of BPA-F is administered before organ removal. The surgical team performs the first incision in the thoracic cavity between ribs 4 and 5 in order to reach the left lung cavity. Lung excision is conducted sequentially (lung restraints, arteries, veins, and left bronchial tubes). The left jugular vein is dissected to be used as an extension of the pulmonary veins as described in the Results Sec. 2.B.1. The lung is then explanted.

In order to preserve organ viability and functionality, the temperature of the explanted lung is lowered from 37 °C to less than 4 °C, and the lung is completely perfused with approximately 1.5 l of Ringer solution and 1 l of preservation HTK-solution (Bretschneider) during 20–30 min. Perfusion is performed through the pulmonary vein. The organ is massaged manually to favor perfusion of the entire organ. After this procedure, the organ is ready to be transported in a double sealed bag inside a refrigerated box to the irradiation facility at the RA-3 reactor.

The time needed to go from the surgery room to the RA-3 reactor is approximately 40 min. In this interval of time, the medical physics team can make minor adjustments to the treatment plan to take into account specific organ characteristics. The irradiation is performed to reach the prescribed dose in the shortest possible time in order to preserve lung integrity and to maximize therapeutic advantage by reducing background dose (fast neutron dose ~1.5 cGy h^{-1}–gamma dose rate 5.0 ± 0.5 Gy h^{-1}).

After treatment, the irradiated lung is transported in a container designed *ad hoc* back to the operating room where the surgical team has prepared the patient to receive the treated organ. Then, the patient is moved to the critical care unit for recovery and follow-up. The total time from the operating room to the reactor and back by car, plus irradiation, is approximately 110 min.

Our working hypothesis is that the ovine lung is a suitable preclinical model for human lung. The anatomical and functional similarities between human lung and sheep lung have been reported, in addition to the similarities in the patterns of repair and regeneration.[15] Studies in sheep have served to elucidate lung physiology in health and disease. In particular, sheep models of respiratory diseases have served for both basic and applied studies of disease and treatment.[16] The size of the sheep allows for the use of equipment and procedures employed in human medicine, contributing to the translation of results from sheep to bedside.[16,17] Within this context, eight surgical procedures were performed to tune surgical and autotransplant procedures. The need to use extensions and/or prostheses for veins, arteries, trachea, and bronchus was studied. The corresponding procedure was established and tested as appropriate in each case.

2.A.2. Experimental measurements in the animal model

Healthy lung is the only organ at risk in the *ex situ* treatment. Thus, the quantitative knowledge of the boron concentration in this organ is mandatory to calculate the absorbed dose and to determine the treatment time. Since taking lung biopsies during treatment may jeopardize the success of the surgical procedure, it is essential to use data previously obtained in a suitable animal model that can reproduce both qualitatively and quantitatively the behavior of the boron compound in human lung.

Two kinds of boron biodistribution studies were performed in the healthy sheep: the first set involved pharmacokinetic studies without lung excision and the second set consisted of evaluation of boron concentration in the explanted and perfused lung. Several samples were taken in each procedure and processed by acid digestion for boron measurement by induced coupled plasma optical emission spectroscopy (ICP-OES) or induced coupled plasma mass spectroscopy (ICP-MS).

2.A.2.a. Pharmacokinetic studies of BPA-F. Biodistribution studies were performed in three adult normal sheep (weight 37 ± 7 kg) using a 0.14M solution of BPA (Interpharma Praha, a.s.)-fructose, prepared as reported by Yoshino *et al.*[18] and in the same way as in projected human treatments. A dose of 350 mg ^{10}B-enriched BPA (>99% ^{10}B) per kilogram of body weight (bw) was infused intravenously during 45 min in previously sedated animals. The choice of this BPA-F dose and administration protocol was based on the BPA-F administration protocols employed in clinical trials worldwide for melanoma,[19] glioblastoma,[20] mesotheliomas and metastasis in the lung,[7,8] and in an experimental model of lung metastases in rat.[21] The animals were kept alive under general anesthesia and connected to a ventilator until the end of the study. During 300 min after the start of the infusion, samples of blood, left lung, skin, and muscle were taken following the sampling time scheme shown in Fig. 1.

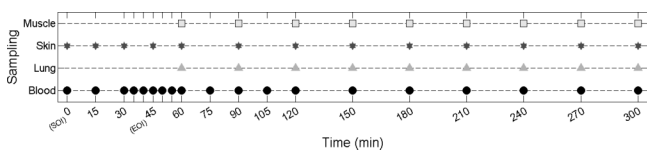

FIG. 1. Sampling time scheme for blood, lung, muscle, and skin used in the BPA-F pharmacokinetic biodistribution studies in the adult sheep model. SOI and EOI indicate start and end of infusion, respectively.

Once the kinetics study was completed, euthanasia was performed by the surgical team according to the UM bioethical protocols. At this point, several samples from other relevant tissues such as heart, diaphragm, kidney, bone, and liver were also taken.

Blood boron concentration-time profiles were fitted using an open two-compartment model.[22] In this model, the central compartment represents the blood and very well-perfused tissues and the peripheral compartment represents poorly perfused regions of the body. Assuming that lung and skin do not exchange directly with each other, the kinetics of each tissue was determined based on the modeled blood boron concentration profile and the model presented in Chuang.[23] Rate constants were estimated from Eq. (13) in Ref. 23 by the nonlinear least square regression method. Prediction bounds with a confidence level of 0.95 were also computed using MATLAB R2013a.[48]

In order to analyze the relation between the boron uptake in lung and in blood, lung-to-blood and skin-to-blood boron concentration ratios as a function of time were calculated based on the fitted profiles.

2.A.2.b. BPA-F retention studies in the explanted lung. While the aim of the experiment described above was to study the behavior of boron concentration as a function of the time after the start of the infusion, another experiment was necessary to assess the absolute boron concentration in lung after excision and perfusion. In fact, the perfusion process was expected to wash out part of the boron accumulated in the tissues.

BPA-F retention studies were carried out in two of the three animals of BPA-F kinetics mentioned above. Given that the left lungs were used for kinetic studies, retention experiments were performed using the right normal lung.

The right lungs were excised 300 min after the start of the infusion. In both studies, six tissue samples were taken prior to perfusion to assess boron concentration before perfusion (bp) and to compare absolute boron uptake between left and right lungs. After perfusion (ap), over 120 samples were taken in total considering the two animals. Boron concentration was later measured by ICP in order to determine the distribution of the boron retention factor (f_R), defined as

$$f_R = \frac{B_{\mathrm{ap}}}{B_{\mathrm{bp}}}, \tag{1}$$

where B_{ap} is the boron concentration in each sample after the perfusion procedure and B_{bp} is the predicted boron concentration value right after lung excision, used to estimate the boron concentration value before perfusion.

2.B. Results of Stage I

2.B.1. Optimization of the surgical procedure

Eight autotransplant surgical experiments were necessary to establish a reliable and reproducible surgical procedure. The time required to perform the complete excision of the lung was reduced from 160 min in the first experiment to an average of 80 ± 30 min in the last three procedures. The anesthetic procedure was adjusted to enable unilateral lung ventilation and subsequent reimplantation. A pivotal stage of the surgical procedure, required to enable successful reimplantation of the organ in the same animal, was the use of bench surgery to extend pulmonary veins through anastomosis of a portion of the jugular vein, extend the pulmonary arteries through anastomosis of polyester prosthesis, and extend bronchi through anastomosis of silicone prosthesis. The reimplantation procedure involved sequential anastomosis of the pulmonary artery, pulmonary veins, and bronchi.

2.B.2. Boron measurements in the animal model

2.B.2.a. Results of BPA-F pharmacokinetic studies. Figures 2(a)–2(c) show the measured boron concentration-time profiles with the model fits for blood, lung, and skin of each studied animal. Prediction bounds with a confidence level of 0.95 were also included. As can be observed, the shape of the curves is very similar for the three animals, the relative

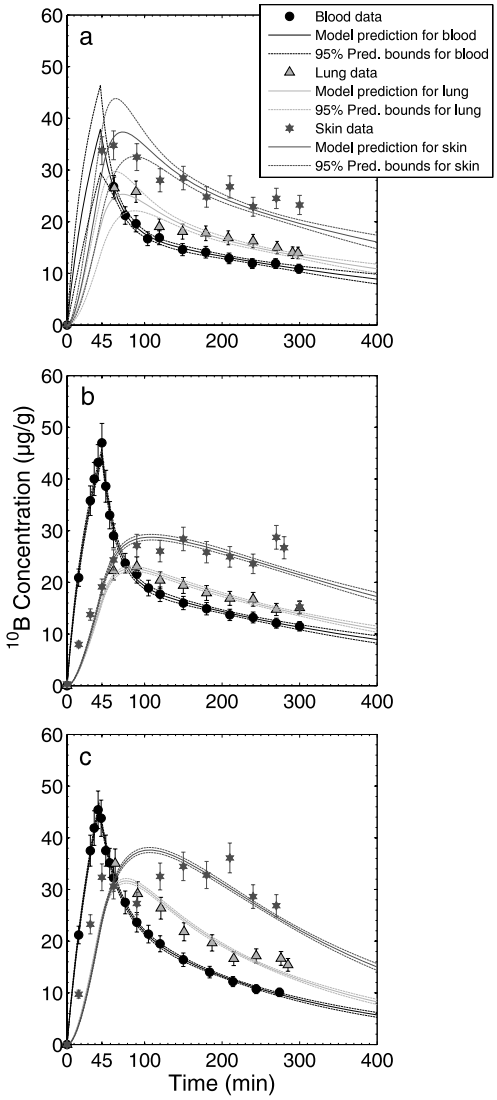

FIG. 2. Measured boron concentration-time profiles with the model predictions for blood, lung, and skin of each animal. Experimental errors of ±8% and prediction bounds with a 95% confidence level are also shown.

behavior between tissues being the same in each case (i.e., the boron concentration in the skin is slightly higher than that of the lung, and both are higher than the concentration in blood).

The blood concentration peaks at the end of infusion (EOI) to about 37.9 ± 9.5, 44.8 ± 1.0, and 46.0 ± 0.7 μg/g, respectively, and drops thereafter, exhibiting the expected biphasic clearance profile. The maximum blood boron concentration in lung is achieved around 50 min after the EOI with an absolute value in the range of 21.8 ± 0.4 μg/g, for all animals. Eighty minutes after EOI, blood, lung, and skin boron concentrations begin to decline slowly and progressively. The smoothness of the three measured boron concentration-time profiles in lung strongly suggests that the distribution of the boron compound is spatially homogeneous in the organ. Note that lung tissue sampling over time is carried out to cover very different locations of the organ.

In order to condense the information of the sheep pharmacokinetic studies in a suitable manner to perform comparisons with humans and dosimetric calculations, the average measured pharmacokinetic profiles for the three animals with the corresponding fits were also computed and are depicted in Fig. 3(a). Based on these results, lung-to-blood and skin-to-blood boron concentration ratios as a function of time were calculated and the resulting profiles are plotted in Fig. 3(b).

Previous biodistribution studies in humans using a BPA-F dose of 350 mg BPA/kg bw showed that (a) the boron average values in blood 60 min after the end of infusion are around 20 μg/g,[24] (b) the boron uptake in healthy lung is nearly the same as the concentration in blood,[25] and (c) the boron uptake in skin is one to two times the concentration in blood.[20,26,27]

Figure 3(a) shows that the average absolute value of the boron concentration in blood for the animal model 60 min after the end of infusion is 18.9 ± 0.6 μg/g, very similar to the one observed in humans. Moreover, the pharmacokinetic model parameters for measured blood in the sheep of $k_1 = 0.022 \pm 0.008$ min^{-1}, $k_2 = 0.012 \pm 0.002$ min^{-1}, $k_3 = 0.007 \pm 0.002$ min^{-1}, and $V = 0.247 \pm 0.048$ (kg/kg) agree well quantitatively with the human data from Kiger *et al.*[22] Lung-to-blood and skin-to-blood boron concentration ratios of 1.3 ± 0.1 and 1.9 ± 0.1 are observed 80 min after EOI [Fig. 3(b)]. These values closely resemble those reported for humans.[28] In addition, lung-to-blood boron concentration ratio shows consistency with the ratios derived from blood and lung boron concentrations reported by Kulvik *et al.*[29] on large animals (Beagle dogs). These findings would support the hypothesis that the large animal serves as a suitable model of the boron biodistribution in humans. In addition, the fact that the lung-to-blood ratio remains almost constant 80 min after EOI allows the blood boron concentration to be used as a surrogate and indirect quantification of boron in the healthy lung for the *ex situ* procedure.

Boron kinetic studies ended at 300 min after the start of the infusion. At this time, the right lung was excised to continue with BPA-F retention studies in the explanted organ. The animals were then sacrificed according to bioethical regulations and additional samples of different tissues of interest were taken for posterior analysis. Boron concentration measurements in these samples are presented and discussed in the Appendix.

2.B.2.b. Results of BPA-F retention studies in the explanted healthy lung. This experiment was performed to evaluate the absolute boron concentration in lung after excision and perfusion of the organ with the preservation solution, employing the boron retention factor f_R given by expression (1) as the end-point. As mentioned in Subsection 2.A.2, tissue samples of the sheep right lung were taken prior to perfusion to evaluate boron concentration before perfusion.

Figure 4 presents the results obtained for the right lungs and includes the corresponding boron concentration interval derived from the left lung measurements, for comparison. Results show that the boron concentration in right lungs prior to perfusion matches the values obtained in the left lungs,

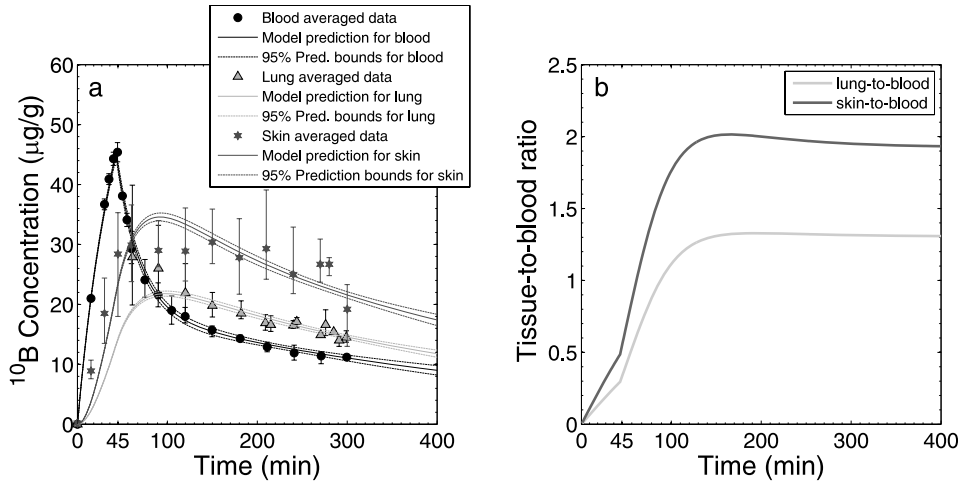

FIG. 3. (a) Average measured boron pharmacokinetic profiles of blood, lung, and skin for the three animals with the corresponding fits. The two-compartment model (Ref. 22) rate constants for blood are $k_1 = 0.022 \pm 0.008$ min^{-1}, $k_2 = 0.012 \pm 0.002$ min^{-1}, $k_3 = 0.007 \pm 0.002$ min^{-1}, and $V = 0.247 \pm 0.048$ (kg/kg). Model parameters of Eq. (13) in Ref. 23 are $K_{1L} = 0.014$ and $K_{2L} = 0.013$ for lung, and $K_{1S} = 0.024$ and $K_{2S} = 0.0145$ for skin. The bars represent the range between minimum and maximum measured values. Prediction bounds with a 95% confidence level are also included. (b) Lung-to-blood and skin-to-blood boron concentration ratios as a function of time based on the results predicted by the model.

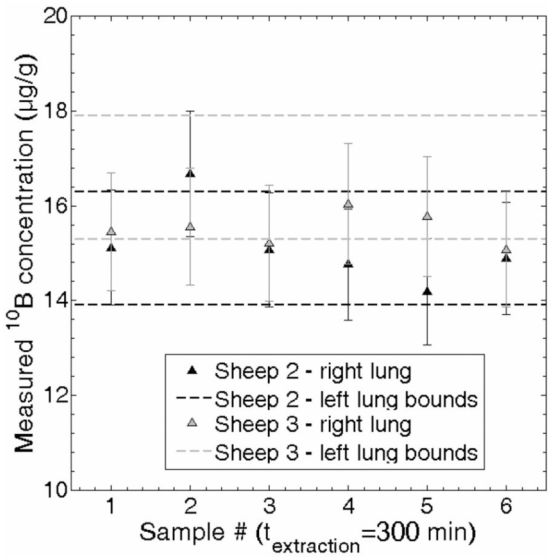

FIG. 4. Comparison of ^{10}B concentration measurements in left and right lungs at excision time t_a for sheep 2 and 3. Left lung bounds correspond to the average of the measured values at t_a with ±8%.

suggesting that the boron uptake in the whole organ is uniform. The fact that the boron uptake in both lungs can be considered the same allows the use of the predicted boron concentration value right after organ excision as an adequate and robust estimate of B_{bp} in Eq. (1).

The boron concentration of more than 120 right lung samples was measured to estimate the distribution of the BPA-F retention factors after performing organ perfusion procedures. Figure 5 presents the empirical distribution of retention factors obtained and its corresponding fit using a log-normal distribution.

While the boron concentration in the lung was homogeneous prior to perfusion, the outcome of the retention factor analysis shows that, as a consequence of perfusion, the final spatial distribution of boron in the healthy lung is not uniform. However, the fact that the expected retention factor with a 68% confidence interval is 0.46 ± 0.14 would suggest that a great portion of the lung volume retains about half the preperfusion boron concentration.

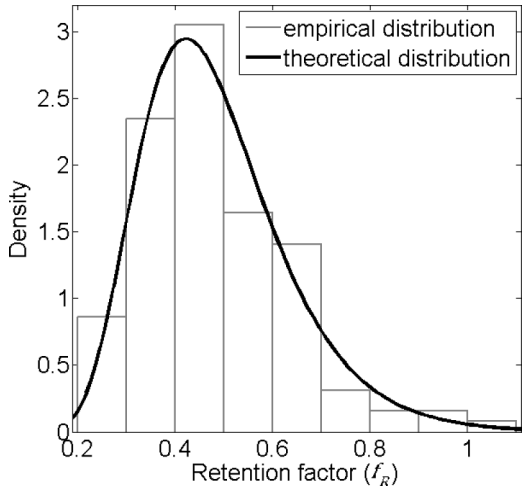

FIG. 5. Distribution of the boron retention factors in explanted lung based on 128 samples from two animals.

Trivillin *et al.*[21] studied the boron retention factor in the small animal lung metastases model used to evaluate BNCT therapeutic potential for lung tumors. The fact that boron washout would also occur in tumor must be taken into account when performing dosimetric calculations. The expected retention factor of 0.46 ± 0.14 determined in the sheep normal lung shows consistency with the preliminary retention factors obtained in the rat model for healthy lung and tumor, of 0.33 ± 0.31 and 0.49 ± 0.18, respectively. The washout in healthy lung would seem to be greater (albeit not significantly) than in tumor in the rat. If confirmed, this would be an asset in terms of improving the tumor/lung boron concentration ratios. However, technical restrictions associated to lung perfusion in a small animal model might cause the organ to retain excess fluid and artificially enhance the reduction in boron concentration in healthy lung. As a more conservative approach, the same retention factor for tumor and healthy lung was assumed in this work.

3. STAGE II: COMPUTATIONAL DOSIMETRY AND CLINICAL ASSESSMENT IN HUMANS

3.A. Materials and methods

The second part of the preclinical assessment is dedicated to the dosimetric calculations in the explanted human lung based on the data derived from large animal experiments carried out in Stage I. The description of the neutron source of RA-3 reactor and the shape of the human lung in the treatment position are also needed to compute the dose delivered to the organ. It is worth noting that there are no available data on the dose constraints for whole lung irradiation in a mixed neutron-photon field (in fact, evaluation of radiotolerance levels is presently ongoing in the context of our project). Therefore, parameters used for dosimetry purposes were thus derived from similar procedures reported in the literature using photons alone, as explained below.

3.A.1. Neutron source

BNCT dosimetry was performed by stochastic neutron and photon transport estimation in space using the Monte Carlo transport code MCNP5 v1.6 (Los Alamos).[30] This approach required the previous knowledge of the particle source and the geometry description of the setup.

CNEA has an open-pool research reactor, RA-3, located in Ezeiza 30 km from the city of Buenos Aires that is equipped with an irradiation facility optimized for the neutron irradiation of explanted organs. A TCCF was built in the RA-3 reactor 8 yr ago, consisting in a rectangular air cavity (~2500 cm^3) surrounded by graphite, giving place to a quasihomogeneous high thermal flux of about 10^{10} cm^{-2} s^{-1}. RA-3 TCCF has been first described and validated in MCNP code by Bortolussi *et al.*[31] and then optimized and updated by Farías *et al.*[49]

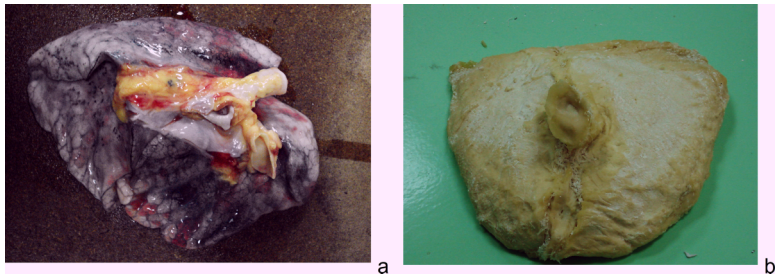

FIG. 6. (a) Adult human collapsed lung of 380 g. (b) Latex phantom of the real human lung.

3.A.2. Geometrical model of a human explanted lung

The configuration of the explanted organ placed in the irradiation position was reproduced in MCNP syntax using a human explanted lung as reference. An adult collapsed lung with a mass of 380 g obtained after complying with the bioethical protocol was used as a model for a geometrically equivalent phantom [Fig. 6(a)]. The organ was covered with plaster in order to obtain a mold that was then filled with a low density (0.9 g cm^{-3}) latex solution [Fig. 6(b)]. The resulting phantom was put inside a double sterile sealed bag and positioned in the irradiation container designed by Gadan *et al.*[32] for *ex situ* protocols at the RA-3 TCCF.

The acrylic device consists in a double wall container that exactly fits in the irradiation facility and passively isolates the organ, reducing the temperature exchange between the experimental setup and the reactor (Fig. 7). The volume of the collapsed lung together with the preservation solution was comparable to that of the container.

A high spatial resolution computed axial tomography ($0.42\times0.42\times1$ mm^3 resolution) of the lung phantom inside the container was acquired to accurately measure the collapsed lung volume (460 cm^3), and consequently, estimate the collapsed lung density (0.86 ± 0.04 g cm^{-3}) by using the mass (380 g). The density of the tissue is important for accurate simulation of the neutron transport in the organ and for a precise dose calculation.

The digitized geometry was segmented into three different regions of interest (i.e., lung, preservation solution, and air) and then translated into MCNP5 code by the MultiCell algorithm, an in-house treatment planning tool that reconstructs the regions in MCNP using adequate syntax and minimizing the number of MCNP subvolumes (cells).[33] Material composition for adult healthy lung was taken from ICRU 46 (Ref. 34) while the preservation solution was described as water. The obtained reconstructed geometry consisting of the lung inside the irradiation device was then inserted into the MCNP model of the reactor, in the TCCF (Fig. 8). The position of the organ was changed according to the different treatment plans evaluated to obtain the best irradiation conditions.

3.A.3. Prescription dose for healthy lung

There are no guidelines available on dose constraints regarding whole lung irradiation using a mixed neutron-photon field. Thus, treatment dose prescriptions must be taken from the literature considering the most similar irradiation

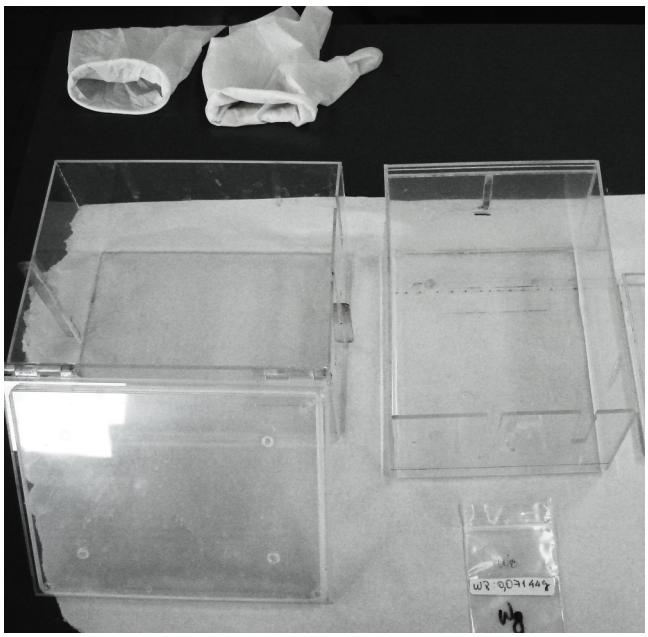

FIG. 7. Double wall acrylic container for irradiation of explanted organs. The air between the walls improves the isolation of the organ, helping to keep the temperature low during irradiation. The dimensions of the container ensure a fixed and reproducible irradiation position coupled to easy handling of the setup during the irradiation.

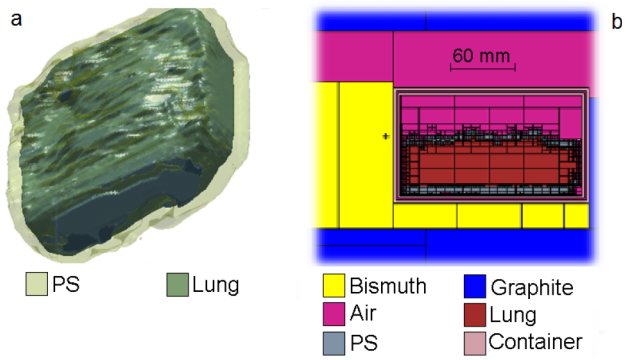

FIG. 8. 3D representation of the geometry adopted by the collapsed human lung with the preservation solution (PS) inside the acrylic container (a), and longitudinal midplane view of the TCCF MCNP model including the MultiCell explanted lung and preservation solution representations inside the acrylic container (b).

protocols applied clinically. Dose-effect studies of whole lung irradiation with photons reported in Van Dyk[35] to treat Ewing Sarcoma metastasis applying antero–posterior rectangular fields represent the most similar scenario to infer dose constraint recommendations for a WLI single fraction. Following Van Dyk's work, a mean lung dose of 7.5 Gy was set as the prescription dose in the treatment of the explanted lung. This dose level was found to be safe in terms of avoiding radiation pneumonitis complications.

3.A.4. Boron concentration in healthy lung and tumor tissue

The sheep preclinical results (Stage I) showed that at about 120 min from the start of infusion, blood, lung, and skin boron concentration profiles show a slow and progressive decline, resulting in almost constant lung-to-blood and skin-to-blood ratios from that time on. Once the surgical procedure was optimized, it was possible to complete the excision of the lung approximately at the time when the slow clearance phase starts (i.e., 120 min from start of infusion). Thus, the boron concentration values for dosimetric calculations in humans were estimated considering an excision time t_a equal to 120 min.

The boron concentration in the healthy lung during the explanted period (B_{ex}) was estimated by multiplying the predicted boron concentration in lung just before excision [i.e., $B_{\mathrm{ba}}(t_a = 120) = 21.4 \pm 0.4\ \mu$g/g (see Fig. 3)] by the mean value of the retention factor reported in Sec. 2.A.2. The obtained value was $B_{ex} = 9.8 \pm 3.0\ \mu$g/g .

Due to the fact that a model of lung tumor in an immunocompetent large animal is not available, boron tumor concentrations cannot be obtained from the preclinical ovine model. However, other research groups reported tumor-to-normal boron concentration ratios (T:N) based on a colon carcinoma diffuse lung metastases model in small animals[21,36] that could be used as an initial educated guess for dosimetric calculations. Moreover, published data of T:N ratios are also available from studies on BNCT of mesothelioma patients.[7,8]

Table I summarizes T:N boron concentration ratios published in the literature. Since these ratios are most likely time dependent, the time from end of infusion to T:N evaluation was indicated. Values range from 1.6 to more than 3. Considering that the inclusion criteria in BNCT usually establish a T:N ratio greater than 2,[5,38,39] and assuming that the ratio between concentration in tumor and in healthy lung does not change due to organ perfusion, values between 2 and 3.5 were assumed for tumor dosimetric calculations in this work.

3.A.5. Calculation of photon-equivalent doses and dosimetry

The standard procedure to estimate photon-equivalent dose in BNCT is to multiply each absorbed dose component by fixed factors that account for the different biological effects caused by high and low LET radiations (RBE factor) and the influence of the boron compound microdistribution (compound biological effectiveness or CBE factor) for the boron component of the dose.[1] To compute the four main contributions to the total dose, it is usual to assume charged particle equilibrium everywhere in the medium so that absorbed doses can be estimated by KERMA.[40] For the calculations, molecular binding effects of hydrogen in the biological materials were taken into account using the $S(\alpha,\beta)$ thermal scattering treatment for hydrogen in light water at 300 K.[40]

In this work, absorbed doses were calculated using the MCNP5 tally f4 (fluence tally) integrated against energy-dependent neutron or photon KERMA factor tables. Lung KERMA factors for neutrons were derived from ICRU 63 KERMA tables[41] (for ^{1}H, ^{12}C, ^{14}N, ^{16}O, and ^{31}P) together with cross section and Q values (for S and Cl) from JENDL-3.2.[42] For photons, x-ray mass attenuation coefficient tables based on data by Hubbel and Seltzer[43] were used. For the boron component, the KERMA factor table for a 1 μg/g concentration reported in Goorley *et al.*[40] was employed.

RBE and CBE factors used to estimate photon-equivalent doses in normal and tumor tissues were those evaluated by Kiger *et al.*[44] for early breathing rate increases in healthy racine lung and those from Coderre *et al.*[45] for 1% surviving fraction in 9 l rat gliosarcoma, using the boron carrier BPA-F (Table II). In the present work, only the endpoint that corresponds to early radiation effects was considered because an acute toxicity would be the most immediate concern in patients.

Healthy lung dose was assessed by dose–volume histogram (DVH) analysis. Mean boron concentration B_{ex} was used to calculate the treatment time necessary to reach the prescription dose. To analyze tumor doses, a theoretical case of multiple lung metastases with lesions in unknown positions was considered. Ten nonoverlapping spherical nodules were randomly generated inside the volume of the lung with density the same as the measured collapsed lung. Sizes of

TABLE I. Tumor-to-normal lung ^{10}B concentration ratios (T:N) for BPA-F reported by different research groups.

Reference	T:N ratio	Time from end of infusion to T:N evaluation (h)	Tumor
Trivillin *et al.* (Ref. 21)	1.9	3.0	Colon ca. mets in rat
Bortolussi *et al.* (Ref. 36)	>3	4.0	Colon ca. mets in rat
Suzuki *et al.* (Refs. 7 and 8)	2.0–3.1	N/A–1.0	Mesothelioma in human
Suzuki *et al.* (Ref. 37)	1.6	0.5	Mesothelioma in rats
Suzuki *et al.* (Ref. 8)	3	1.0	Lung mets in human

TABLE II. RBE and CBE factors used to compute photon-equivalent doses in normal and tumor tissues.

	$^{10}B(n,\alpha)^{7}Li$	$^{14}N(n,p)^{14}C$	Fast neutrons	Photons
Healthy lung	1.4 (Ref. 44)	3.2 (Ref. 45)	3.2 (Ref. 45)	1
Tumor	3.8 (Ref. 45)	3.2 (Ref. 45)	3.2 (Ref. 45)	1

the lesions were sampled between 0.2 and 19 cm^3 from a normal distribution with a mean of 3.3 cm^3. This process was repeated 1000 times to cover the whole lung. For each trial, the expected fraction of controlled lesions (i.e., the arithmetic mean of the TCPs for the ten lesions) was computed. The tumor control probability model for lung cancer extended to the case of BNCT in Farías *et al.*[33] was used in calculations. This TCP model relies on the Hug-Kellerer survival model for a multifraction regime and accounts for nonuniform dose distributions.[46,47]

3.B. Results of Stage II

3.B.1. Treatment planning and irradiation time

The goal of the treatment planning was to maximize the tumor dose without exceeding the prescription dose to the healthy tissue (i.e., a mean lung dose equal to 7.5 Gy_w). Considering that a clinical scenario of multiple lung metastases with lesions in unknown positions was proposed, increasing the homogeneity of the delivered dose to the lung would enhance the probability that all the lesions would receive a potentially therapeutic dose. To this end, a rotation of 180° (about the vertical axis) halfway through the irradiation time was proposed. This configuration compensates the neutron flux attenuation in depth inside the organ, keeping dose heterogeneity as low as possible in the entire lung volume.

Assuming that the mean boron concentration in the explanted organ ($B_{ex} = 9.8 \pm 3.0\ \mu g/g$) remained constant during the whole *ex situ* period, and that the total irradiated volume is healthy lung, the irradiation time required to achieve the prescription dose was 415 ± 5 s.

3.B.2. Dosimetrical outcome and evaluation

Figure 9(a) shows the cumulative DVH obtained when the whole explanted organ is considered healthy lung, for the expected value of the boron concentration after perfusion ($B_{ex} = 9.8\ \mu g$ / g) and for the upper bound of the ^{10}B concentration interval ($B_{ex} = 12.8\ \mu g/g$). It also includes the cumulative dose–volume histogram as a function of the tumor-to-normal tissue boron concentration ratio if the entire lung is hypothetically considered tumor.

The cumulative dose–volume histogram obtained in healthy lung for $B_{ex} = 9.8\ \mu g/g$ derives, as expected, a mean lung dose of 7.5 Gy_w (i.e., the value to avoid radiation pneumonitis complications). However, if a $B_{ex} + \Delta B_{ex}$ is considered for dose calculations, the mean dose is 8.4 Gy_w, a value that would still be acceptable with a low probability (~5%) of inducing radiation pneumonitis. Mean lung dose is composed of 3.1, 2.1, 0.5, and 1.8 Gy_w due to boron, thermal neutron, fast neutron, and photon dose components, respectively.

As depicted in Fig. 9(a), the maximum dose delivered to lung is considerably lower than the minimum dose delivered to tumor even for the minimum T:N ratio allowed by the inclusion criteria. This dosimetric advantage results from tumor selective boron uptake and microdistribution of the boronated compound in tumor.

In order to evaluate the therapeutic potential of BNCT for the treatment of metastatic dissemination in the lung, a more realistic clinical scenario of ten lesions spread in the organ was considered. The probability of controlling each nodule was computed based on the TCP model for single fraction and inhomogeneous doses in Farías *et al.*[33] The expected number of controlled nodules for T:N boron concentration ratios ranging from 2 to 3.5 is shown in Fig. 9(b). The average fraction of controlled nodules (expressed as a percentage) is higher than 85% for the lowest T:N ratio considered in the analysis. This expected fraction increases with the T:N ratio,

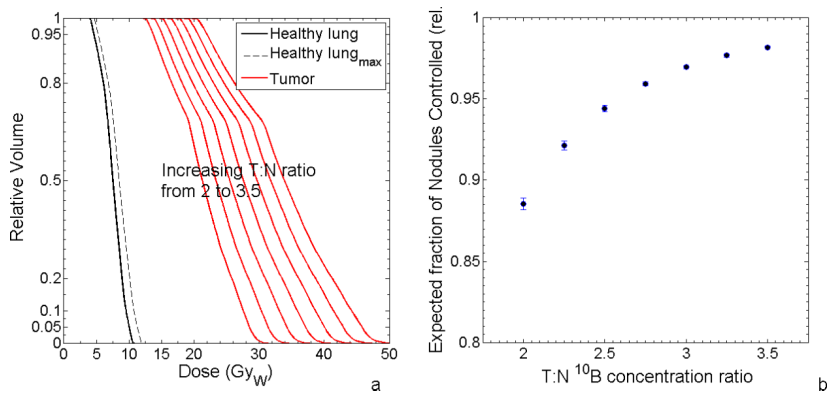

FIG. 9. (a) Cumulative dose–volume histograms obtained in human lung, considering the entire volume as healthy tissue or as tumor. Solid and dotted black lines show DVH in normal lung for $B_{ex} = 9.8\ \mu g/g$ (the mean value) and for $B_{ex} = 12.8\ \mu g/g$ ($B_{ex} + \Delta B_{ex}$). The set of solid lines to the right side of the figure shows DVH in tumor for T:N from 2 to 3.5. (b) Average fraction of nodules controlled as a function of the tumor-to-normal boron concentration ratio, for a fixed healthy lung dose constraint.

reaching a value as high as 97% for a 3.5 T:N ratio. These results strongly suggest that even for low values of tumor-to-normal boron concentration ratios, there are good chances that most of the nodules are controlled.

4. DISCUSSION AND CONCLUSIONS

This work addresses the preclinical requirements and the feasibility of BNCT for the treatment of diffuse lung tumors considering a novel *ex situ* irradiation procedure. A large animal model based on normal adult sheep to assess boron biodistribution and surgical feasibility was implemented and validated for preclinical BNCT for the first time.

The preclinical model contributes to the knowledge of the potential complications and limitations of the lung autotransplantation surgery that could conceivably occur in human patients. This knowledge is pivotal to the development and optimization of this novel technique, prioritizing safety and therapeutic efficacy.

BPA-F biodistribution studies performed with normal adult sheep showed that the boron kinetics in blood, lung, and skin would adequately represent the boron behavior and absolute uptake expected in human tissues and afforded values that can be used in dosimetric calculations. The study of boron kinetics in a single large animal by successive sampling affords a "true to life" kinetic profile. Conversely, in the case of the widespread biodistribution studies performed in small animals, the kinetic profile is reconstructed from the data corresponding to different sets of animals euthanized at different times. Results of the measured boron concentration-time profiles strongly suggest that the distribution of the boron compound is spatially homogeneous in the lung. The fact that the lung-to-blood ^{10}B ratio remains almost constant at the time the slow clearance phase starts, would allow the blood boron concentration to be used as a surrogate and indirect quantification of the estimated boron concentration in the explanted healthy lung. A constant lung-to-blood ratio of 1.3 ± 0.1 was observed from 80 min after the end of BPA-F infusion. This ratio obtained in the present study would be very valuable in a clinical scenario due to the complexity and sometimes the impossibility to measure lung boron concentration during the treatment. It is noteworthy that biodistribution studies were performed using both lungs, making the results equally valid for the left and right lungs.

The proposed preclinical animal model also allowed for the study of the explanted lung. The boron concentration was expected to fall as a result of the application of the preservation protocol required to preserve the function of the treated lung to be reimplanted. The distribution of the boron concentration retention factor after organ perfusion was obtained for healthy lung. The mean retention factor obtained in this work of 0.46 ± 0.14 is within the same range as the values reported by Trivillin *et al.*[21] for metastatic colon carcinoma model in rat perfused lung. Considering that in the small animal model the tumor retention factor was about the same as that observed in the normal sheep lung, assuming a unique value for both tissues in humans seemed a reasonable and conservative starting point.

The novel insights derived from this work were nonexistent to date and are absolutely necessary to start the radiotolerance study of the lung using mixed neutron-photon field irradiation with BNCT. In addition, supplementary boron concentration data reported in the Appendix for other organs and tissues beyond those considered relevant for the *ex situ* procedure would contribute to the feasibility assessment and dosimetric analysis of BNCT for tumors localized in the thorax. Moreover, all the presented results are essential to perform an accurate and safe dosimetry in patients.

A detailed computational representation of the geometry of the lung was built based on a real collapsed human lung. Dosimetric calculations and dose limiting considerations were based on the experimental measurements specifically tailored for the *ex situ* irradiation procedure, and on the most suitable information published in the literature. In addition, a workable treatment plan and expected operative constraints were considered to assess the clinical application of *ex situ* BNCT for lung tumors at the RA-3 reactor in Argentina in the most realistic scenario possible.

A theoretical case of multiple lung metastases with lesions in unknown positions was proposed and analyzed for *ex situ* BNCT in this work. This selected case is not well suited for locoregional therapies such as photon therapy or surgery. Calculations revealed that if the *ex situ* whole lung BNCT irradiation strategy was employed, the expected fraction of controlled lesions would be promising, i.e., over 85%, even for the lowest tumor-to-normal boron concentration ratio considered (T:N = 2). The endpoint for calculations corresponds to early radiation effects because acute toxicity would be the most immediate concern in patients. However, if late radiation effects are taken into account (i.e., if a CBE factor for late functional effects of 2.3 is assumed for calculations), the average fraction of controlled nodules is still promising, reaching a value higher than 80% for a T:N ratio of 2.5.

The most frequent clinical scenario for lung metastases in humans is dissemination in both lungs. In this case, the procedure of *ex situ* irradiation may be performed sequentially, with an appropriate time between irradiations for the first treated lung to recover. The results obtained in the theoretical case are expected to hold true for both lungs. Based on the results and lessons learned from this work, the general procedure proposed for humans is almost the same to the one described for animals but including some additional steps that allow for a tailored treatment plan to be designed for each patient. As in the case of melanoma treatments carried out in Argentina, patients will be intravenously infused with BPA-F (350 mg kg^{-1} bw) over 90 min. During this time and half the period needed for lung explantation, blood samples will be extracted in spans of 10–15 min. While the surgical team continues to work on the organ explantation, the ^{10}B concentration in blood will be analyzed by ICP-OES. The estimated blood boron concentration value immediately before the organ excision will be used as a surrogate of the boron concentration in the healthy tissue of

the explanted lung. A constant lung-to-blood ratio of 1.3 ± 0.1 and a mean retention factor 0.46 ± 0.14 will be assumed for dosimetry calculation purposes. Just before the explanted lung is transported to the irradiation facility, a CT study of the organ inside the acrylic container can be carried out in the same building. The time elapsed between when the organ leaves the operating theatre and is ready for irradiation is about 55 min. In this interval of time, a tailored treatment plan that takes into account specific organ characteristics obtained from the CT study can be performed. Note that the Multicell reconstruction in combination with the MCNP estimations can be carried out in less than 40 min using an optimized source representation of the FCCT and parallel computing (with 40 Intel® i7 processors). Finally, adjustments to the final value of the irradiation time may be performed, if needed.

Whole lung irradiation for tumor spreads in the case of Wilms or Ewing metastases has been performed with promising results, as stated in recent publications by Whelan *et al.*[13] and Bölling *et al.*[12] Considering these cases, the clinical application of *ex situ* BNCT as a concomitant treatment may be expected to result in similar lung toxicity with at least the same good overall survival. Note that for the same lung toxicity that is acceptable in the mentioned standard applications, the proposed BNCT treatment would deliver a higher dose selectively to the tumors in a single fraction.

Collectively, the results and analysis presented in this work would strongly suggest that *ex situ* BNCT is a feasible and highly promising technique that could greatly contribute to the treatment of metastatic lung disease in those patients without extrapulmonary spread, increasing not only the expected overall survival but also the resulting quality of life.

APPENDIX: BPA-F PHARMACOKINETIC STUDIES: OTHER RELEVANT TISSUES

Boron concentration measurements in additional tissues of clinical relevance for *in situ* lung irradiation or, more generally, for BNCT of tumors localized in the thorax are presented in this appendix.

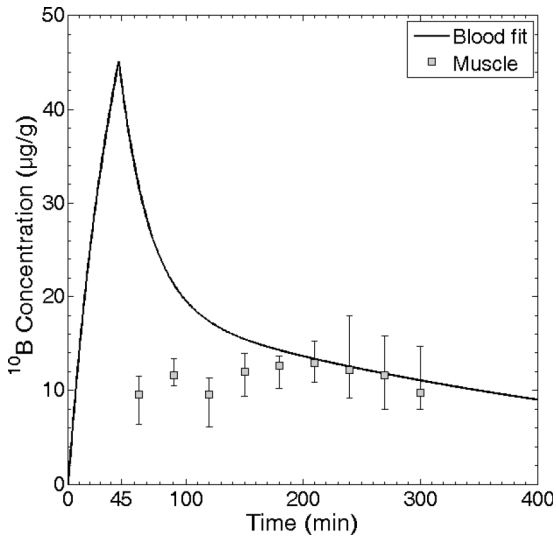

FIG. 10. Average measured boron pharmacokinetic profile of muscle for two animals with the model prediction for blood. The bars represent the range between minimum and maximum measured values.

TABLE III. Boron concentration values of different tissues involved in thorax irradiations with BNCT, at 300 min from the start of BPA-F infusion. Blood, lung, and skin average values are those derived from the fit with confidence interval of 95%. Concentration values for the remaining tissues are reported as average measured value with the minimum and maximum concentration range.

Organ/tissue	^{10}B concentration (μg/g)
Blood (fit)	11.0 [10.5–11.5][a]
Lung (fit)	14.5 [14.2–14.9][a]
Skin (fit)	21.6 [21.0–22.1][a]
Heart ($n = 6$)	16 [10–26]
Esophagus ($n = 3$)	10 [9–11]
Diaphragm ($n = 3$)	21 [19–22]
Liver ($n = 5$)	11 [9–12]
Kidney ($n = 9$)	112 [57–152]

[a]Confidence interval of 95%.

Figure 10 shows the average measured pharmacokinetic profile for two animals corresponding to muscle (soft tissue), with the model prediction for blood. As expected, the muscle boron concentration profile closely follows the blood profile, deriving a muscle-to-blood ratio of about 1 after 150 min from the start of the infusion.

Table III presents the boron concentration obtained at 300 min from the start of infusion, for most of the tissues and organs that would be involved in thorax irradiations with BNCT. Values for blood, lung, and skin are also presented as reference. The fact that boron concentration values in kidney are much higher than those obtained in the other tissues is explained by noting that BPA-F is primarily eliminated by renal clearance.[22]

[a)]R. O. Farías and M. A. Garabalino contributed equally to this work.
[b)]Author to whom correspondence should be addressed. Electronic mail: srgonzal@cnea.gov.ar; Telephone: 54 11 6772-7865; Fax: 54 11 6772-7611.

[1]J. A. Coderre and G. M. Morris, "The radiation biology of boron neutron capture therapy," Radiat. Res. **151**(1), 1–18 (1999).
[2]R. F. Barth, M. G. Vicente, O. K. Harling, W. S. Kiger 3rd, K. J. Riley, P. J. Binns, F. M. Wagner, M. Suzuki, T. Aihara, and I. Kato, "Current status of boron neutron capture therapy of high grade gliomas and recurrent head and neck cancer," Radiat. Oncol. **7**, 146–167 (2012).
[3]A. Zonta, U. Prati, L. Roveda, C. Ferrari, S. Zonta, A. Clerici, C. Zonta, T. Pinelli, F. Fossati, S. Altieri, S. Bortolussi, P. Bruschi, R. Nano, S. Barni, P. Chiari, and G. Mazzini, "Clinical lessons from the first applications of BNCT on unresectable liver metastases," J. Phys.: Conf. Ser. **41**(1), 484–495 (2006).
[4]P. R. Menéndez, B. M. C. Roth, M. D. Pereira, M. R. Casal, S. J. González, D. B. Feld, G. A. Santa Cruz, J. Kessler, J. Longhino, H. Blaumann, R. Jiménez rebagliati, O. A. Calzetta larrieu, C. Fernández, S. I. Nievas, and S. J. Liberman, "BNCT for skin melanoma in extremities: Updated argentine clinical results," Appl. Radiat. Isot. **67**(7–8), S50–S53 (2009).
[5]L. Kankaanranta, T. Seppälä, H. Koivunoro, K. Saarilahti, T. Atula, J. Collan, E. Salli, M. Kortesniemi, J. Uusi-Simola, A. Mäkitie, M. Seppänen, H. Minn, P. Kotiluoto, I. Auterinen, S. Savolainen, M. Kouri, and H. Joensuu, "Boron neutron capture therapy in the treatment of locally recurred head and neck cancer," Int. J. Radiat. Oncol., Biol., Phys. **69**(2), 475–482 (2007).
[6]L. Kankaanranta, T. Seppälä, H. Koivunoro, K. Saarilahti, T. Atula, J. Collan, E. Salli, M. Kortesniemi, J. Uusi-Simola, P. Välimäki, A. Mäkitie,

M. Seppänen, H. Minn, H. Revitzer, M. Kouri, P. Kotiluoto, T. Seren, I. Auterinen, S. Savolainen, and H. Joensuu, "Boron neutron capture therapy in the treatment of locally recurred head-and-neck cancer: Final analysis of a phase I/II trial," Int. J. Radiat. Oncol., Biol., Phys. **82**(1), e67–e75 (2012).
[7]M. Suzuki, K. Endo, H. Satoh, Y. Sakurai, H. Kumada, H. Kimura, S. Masunaga, Y. Kinashi, K. Nagata, A. Maruhashi, and K. Ono, "A novel concept of treatment of diffuse or multiple pleural tumors by boron neutron capture therapy (BNCT)," Radiother. Oncol. **88**(2), 192–195 (2008).
[8]M. Suzuki, O. Suzuki, Y. Sakurai, H. Tanaka, N. Kondo, Y. Kinashi, S. Masunaga, A. Maruhashi, and K. Ono, "Reirradiation for locally recurrent lung cancer in the chest wall with boron neutron capture therapy (BNCT)," Int. Cancer Conf. J. **1**(4), 235–238 (2012).
[9]T. Pinelli, A. Zonta, S. Altieri, S. Barni, A. Braghieri, P. Pedroni, P. Bruschi, P. Chiari, C. Ferrari, and C. Zonta, "TAOrMINA: From the first idea to the application to the human liver," in *Research and Development in Neutron Capture Therapy*, edited by M. W. Sauerwein, R. Moss, and A. Wittig (Monduzzi Editore, International Proceedings Division, Bologna, 2002), pp. 1065–1072.
[10]P. Navarria, F. De Rose, and A. M. Ascolese, "SBRT for lung oligometastases: Who is the perfect candidate?," Rep. Pract. Oncol. Radiother. (2014) (in press).
[11]D. S. Ettinger, W. Akerley, H. Borghaei, A. C. Chang, R. T. Cheney, L. R. Chirieac, T. A. D'Amico, T. L. Demmy, R. Govindan, F. W. Grannis, S. C. Grant, L. Horn, T. M. Jahan, R. Komaki, F.-M. (Spring) Kong, M. G. Kris, L. M. Krug, R. P. Lackner, I. T. Lennes, B. W. Loo, R. Martins, G. A. Otterson, J. D. Patel, M. C. Pinder-Schenck, K. M. Pisters, K. Reckamp, G. J. Riely, E. Rohren, T. A. Shapiro, S. J. Swanson, K. Tauer, D. E. Wood, S. C. Yang, K. Gregory, and M. Hughes, "Non–small cell lung cancer, version 2.2013," J. Natl. Compr. Canc. Netw. **11**(6), 645–653 (2013).
[12]D. T. Bölling, A. Schuck, M. Paulussen, U. Dirksen, A. Ranft, S. Könemann, J. Dunst, N. Willich, and H. Jürgens, "Whole lung irradiation in patients with exclusively pulmonary metastases of ewing tumors," Strahlenther. Onkol. **184**(4), 193–197 (2008).
[13]J. S. Whelan, R. J. Burcombe, J. Janinis, A. M. Baldelli, and A. M. Cassoni, "A systematic review of the role of pulmonary irradiation in the management of primary bone tumours," Ann. Oncol. **13**(1), 23–30 (2002).
[14]M. Miller, J. Quintana, J. Ojeda, S. Langan, S. Thorp, E. Pozzi, M. Sztejnberg, G. Estryk, R. Nosal, E. Saire, H. Agrazar, and F. Graiño, "New irradiation facility for biomedical applications at the RA-3 reactor thermal column," Appl. Radiat. Isot. **67**(7–8), S226–S229 (2009).
[15]The Roslin Institute (University of Edinburgh)–Dr David Collie, available: http://www.roslin.ed.ac.uk/david-collie/gene-therapy-for-cystic-fibrosis/, accessed 11 March 2015.
[16]E. N. Meeusen, K. J. Snibson, S. J. Hirst, and R. J. Bischof, "Sheep as a model species for the study and treatment of human asthma and other respiratory diseases," Drug Discovery Today: Dis. Models **6**(4), 101–106 (2009).
[17]I. C. McMillen, "The sheep-an ideal model for biomedical research?," ANZCCART News **14**(2), 1–4 (2001).
[18]K. Yoshino, A. Suzuki, Y. Mori, H. Kakihana, C. Honda, Y. Mishima, T. Kobayashi, and K. Kanda, "Improvement of solubility of p-boronophenylalanine by complex formation with monosaccharides," Strahlenther. Onkol. Organ Dtsch. Rontgengesellschaft **165**(2–3), 127–129 (1989).
[19]S. J. González, M. R. Bonomi, G. A. Santa Cruz, H. R. Blaumann, O. A. C. Larrieu, P. Menéndez, R. J. Rebagliati, J. Longhino, D. B. Feld, M. A. Dagrosa, C. Argerich, S. G. Castiglia, D. A. Batistoni, S. J. Liberman, and B. M. C. Roth, "First BNCT treatment of a skin melanoma in Argentina: Dosimetric analysis and clinical outcome," Appl. Radiat. Isot. **61**(5), 1101–1105 (2004).
[20]P. M. Busse, O. K. Harling, M. R. Palmer, W. S. Kiger, J. Kaplan, I. Kaplan, C. F. Chuang, J. T. Goorley, K. J. Riley, T. H. Newton, G. A. S. Cruz, X.-Q. Lu, and R. G. Zamenhof, "A critical examination of the results from the Harvard-MIT NCT program phase I clinical trial of neutron capture therapy for intracranial disease," J. Neuro-Oncol. **62**(1–2), 111–121 (2003).
[21]V. A. Trivillin, M. A. Garabalino, L. L. Colombo, S. J. González, R. O. Farías, A. Monti Hughes, E. C. C. Pozzi, S. Bortolussi, S. Altieri, M. E. Itoiz, R. F. Aromando, D. W. Nigg, and A. E. Schwint, "Biodistribution of the boron carriers boronophenylalanine (BPA) and/or decahydrodecaborate (GB-10) for boron neutron capture therapy (BNCT) in an experimental model of lung metastases," Appl. Radiat. Isot. **88**, 94–98 (2014).
[22]W. S. Kiger, M. R. Palmer, K. J. Riley, R. G. Zamenhof, and P. M. Busse, "A pharmacokinetic model for the concentration of 10B in blood after boronophenylalanine-fructose administration in humans," Radiat. Res. **155**(4), 611–618 (2001).
[23]C. F.-Y. Chuang, "Experimental evaluation and mathematical modeling of the pharmacokinetics of boronophenylalanine-fructose (BPA-f) in murine tumor models," Ph.D. thesis, Department of Nuclear Engineering, Massachusetts Institute of Technology, 1999.
[24]L. Kankaanranta, T. Seppälä, H. Koivunoro, P. Välimäki, A. Beule, J. Collan, M. Kortesniemi, J. Uusi-Simola, P. Kotiluoto, I. Auterinen, T. Serèn, A. Paetau, K. Saarilahti, S. Savolainen, and H. Joensuu, "l-Boronophenylalanine-mediated boron neutron capture therapy for malignant glioma progressing after external beam radiation therapy: A phase I study," Int. J. Radiat. Oncol., Biol., Phys. **80**(2), 369–376 (2011).
[25]M. Suzuki, Y. Sakurai, S. Masunaga, Y. Kinashi, K. Nagata, A. Maruhashi, and K. Ono, "Feasibility of boron neutron capture therapy (BNCT) for malignant pleural mesothelioma from a viewpoint of dose distribution analysis," Int. J. Radiat. Oncol., Biol., Phys. **66**(5), 1584–1589 (2006).
[26]H. Fukuda, J. Hiratsuka, T. Kobayashi, Y. Sakurai, K. Yoshino, H. Karashima, K. Turu, K. Araki, Y. Mishima, and M. Ichihashi, "Boron neutron capture therapy (BNCT) for malignant melanoma with special reference to absorbed doses to the normal skin and tumor," Australas. Phys. Eng. Sci. Med. **26**(3), 97–103 (2003).
[27]S. J. Liberman, A. Dagrosa, R. A. Jiménez rebagliati, M. R. Bonomi, B. M. Roth, L. Turjanski, S. I. Castiglia, S. J. González, P. R. Menéndez, R. Cabrini, M. J. Roberti, and D. A. Batistoni, "Biodistribution studies of boronophenylalanine–fructose in melanoma and brain tumor patients in Argentina," Appl. Radiat. Isot. **61**(5), 1095–1100 (2004).
[28]H. Fukuda, C. Honda, N. Wadabayashi, T. Kobayashi, K. Yoshino, J. Hiratsuka, J. Takahashi, T. Akaizawa, Y. Abe, M. Ichihashi, and Y. Mishima, "Pharmacokinetics of 10B-p-boronophenylalanine in tumours, skin and blood of melanoma patients: A study of boron neutron capture therapy for malignant melanoma," Melanoma Res. **9**(1), 75–83 (1999).
[29]M. E. Kulvik, J. K. Vähätalo, J. Benczik, M. Snellman, J. Laakso, R. Hermans, E. Järviluoma, M. Rasilainen, M. Färkkilä, and M. E. Kallio, "Boron biodistribution in beagles after intravenous infusion of 4-dihydroxyborylphenylalanine–fructose complex," Appl. Radiat. Isot. **61**(5), 975–979 (2004).
[30]X-5 Monte Carlo Team, MCNP — A General Monte Carlo N-Particle Transport Code, version 5, Volume I: Overview and Theory, 3 vols, Los Alamos National Laboratory, 2003.
[31]S. Bortolussi, J. M. Pinto, S. I. Thorp, R. O. Farias, M. S. Soto, M. Sztejnberg, E. C. C. Pozzi, S. J. Gonzalez, M. A. Gadan, A. N. Bellino, J. Quintana, S. Altieri, and M. Miller, "Simulation of the neutron flux in the irradiation facility at RA-3 reactor," Appl. Radiat. Isot. **69**(12), 1924–1927 (2011).
[32]M. Gadan, V. Crawley, S. Thorp, and M. Miller, "Preliminary liver dose estimation in the new facility for biomedical applications at the RA-3 reactor," Appl. Radiat. Isot. **67**(7–8), S206–S209 (2009).
[33]R. O. Farías, S. Bortolussi, P. R. Menéndez, and S. J. González, "Exploring boron neutron capture therapy for non-small cell lung cancer," Phys. Med. **30**(8), 888–897 (2014).
[34]International Commission on Radiological Units and Measurements, "Proton and neutron interaction data for body tissues," ICRU Report No. 46 (1992).
[35]J. Van Dyk, T. J. Keane, S. Kan, W. D. Rider, and C. J. H. Fryer, "Radiation pneumonitis following large single dose irradiation: A re-evaluation based on absolute dose to lung," Int. J. Radiat. Oncol., Biol., Phys. **7**(4), 461–467 (1981).
[36]S. Bortolussi, J. G. Bakeine, F. Ballarini, P. Bruschi, M. A. Gadan, N. Protti, S. Stella, A. Clerici, C. Ferrari, L. Cansolino, C. Zonta, A. Zonta, R. Nano, and S. Altieri, "Boron uptake measurements in a rat model for boron neutron capture therapy of lung tumours," Appl. Radiat. Isot. **69**(2), 394–398 (2011).
[37]M. Suzuki, Y. Sakurai, S. Hagiwara, S. Masunaga, Y. Kinashi, K. Nagata, A. Maruhashi, M. Kudo, and K. Ono, "First attempt of boron neutron capture therapy (BNCT) for hepatocellular carcinoma," Jpn. J. Clin. Oncol. **37**(5), 376–381 (2007).
[38]T. Aihara, J. Hiratsuka, N. Morita, M. Uno, Y. Sakurai, A. Maruhashi, K. Ono, and T. Harada, "First clinical case of boron neutron capture therapy for head and neck malignancies using 18F-BPA PET," Head Neck **28**(9), 850–855 (2006).
[39]A. Wittig, M. Malago, L. Collette, R. Huiskamp, S. Bührmann, V. Nievaart, G. M. Kaiser, K.-H. Jöckel, K. W. Schmid, U. Ortmann, and W. A. Sauerwein, "Uptake of two 10B-compounds in liver metastases of colorectal adenocarcinoma for extracorporeal irradiation with boron neutron capture therapy (EORTC trial 11001)," Int. J. Cancer **122**(5), 1164–1171 (2008).

[40]J. T. Goorley, W. S. Kiger III, and R. G. Zamenhof, "Reference dosimetry calculations for neutron capture therapy with comparison of analytical and voxel models," Med. Phys. **29**(2), 145–156 (2002).
[41]International Commission on Radiological Units and Measurements, "Nuclear data for neutron and proton radiotherapy and for radiation protection," ICRU Report No. 63 (2000).
[42]T. Nakagawa, K. Shibata, S. Chiba, T. Fukahori, Y. Nakajima, Y. Kikuchi, T. Kawano, Y. Kanda, T. Ohsawa, H. Matsunobu, M. Kawai, A. Zukeran, T. Watanabe, S. Igarasi, K. Kosako, and T. Asami, "Japanese evaluated nuclear data library version 3 revision-2: JENDL-3.2," J. Nucl. Sci. Technol. **32**(12), 1259–1271 (1995).
[43]US Department of Commerce, "NIST: X-ray mass attenuation coefficients," available: http://www.nist.gov/pml/data/xraycoef/index.cfm, accessed 02 June 2014.
[44]J. L. Kiger, W. S. Kiger III, K. J. Riley, P. J. Binns, H. Patel, J. W. Hopewell, O. K. Harling, P. M. Busse, and J. A. Coderre, "Functional and histological changes in rat lung after boron neutron capture therapy," Radiat. Res. **170**(1), 60–69 (2008).
[45]J. A. Coderre, M. S. Makar, P. L. Micca, M. M. Nawrocky, H. B. Liu, D. D. Joel, D. N. Slatkin, and H. I. Amols, "Derivations of relative biological effectiveness for the high-let radiations produced during boron neutron capture irradiations of the 9l rat gliosarcoma in vitro and in vivo," Int. J. Radiat. Oncol., Biol., Phys. **27**(5), 1121–1129 (1993).
[46]O. Hug and A. Kellerer, "Zur interpretation der dosiswirkungsbeziehungen in der strahlenbiologie," Biophysik **1**(1), 20–32 (1963).
[47]S. J. González and G. A. S. Cruz, "The photon-isoeffective dose in boron neutron capture therapy," Radiat. Res. **178**(6), 609–621 (2012).
[48]MATLAB and Statistics Toolbox Release 2013a, The MathWorks, Inc., Natick, MA.
[49]RA3 Neutron Facility optimization and verification, R. O. Farías, S. Bortolussi, S. Thorp, E. E. C. Pozzi, M. A. Gadan, M. Sztejnberg, M. Miller, S. Altieri, and S. J. González, CNEA Internal Technical Report—2012/01.